



ISS2012

# Numerical simulation of permanent magnet method for measuring critical current density in superconducting film: dominant experimental conditions for crack detection

T. Takayama<sup>a\*</sup>, A. Kamitani<sup>b</sup><sup>a</sup>Faculty of Engineering, Yamagata University, 4-3-16, Johnan, Yonezawa, Yamagata 992-8510, Japan<sup>b</sup>Graduate School of Science and Engineering, Yamagata University, 4-3-16, Johnan, Yonezawa, Yamagata 992-8510, Japan

## Abstract

The scanning permanent magnet method for measuring the critical current density in a high-temperature superconducting (HTS) film has been reproduced numerically. For this purpose, a numerical code has been developed for analyzing the time evolution of a shielding current density in an HTS film with a crack. The results of computations show that the attractive force  $F_r$  and repulsive one  $F_a$  are observed near the endpoints of the crack when the symmetry axis of the magnet approaches the crack. In addition, the both forces,  $F_r$  and  $F_a$ , have the maximum value only when the magnet is located above the crack. This means that the crack size and position can be estimated by using the scanning method.

© 2013 The Authors. Published by Elsevier B.V. Open access under [CC BY-NC-ND license](https://creativecommons.org/licenses/by-nc-nd/4.0/).

Selection and/or peer-review under responsibility of ISS Program Committee.

**Keywords:** Critical currents; Defect detection; Numerical analysis; Permanent magnet; Superconducting films

## 1. Introduction

The practical applications of the high-temperature superconductors (HTSs) require the measurement of a critical current density  $j_C$ . While the standard four-probe method is generally used to measure  $j_C$ , it may lead to degradation of HTS characteristics. For this reason, contactless methods such as the inductive method [1], the hall sensor method [2], and the hall probe method [3] have been proposed. These methods have been applied to the measurement of  $j_C$ -distributions for a large-area samples such as an HTS tape or wire.

Ohshima *et al.* have proposed a novel contactless method for measuring  $j_C$  in an HTS thin film [4]. While moving a permanent magnet above an HTS film, the electromagnetic force  $F_z$  acting on the film is measured. Consequently, they found that the maximum repulsive force  $F_M$  is almost proportional to  $j_C$ . This means that  $j_C$  is estimated from the measured value of  $F_M$ . Hereafter, this method is called the standard permanent magnet method. The standard method is used for the estimation of  $j_C$ -distributions [5] or the detection of any cracks containing in an HTS tape [6]. However, it necessary to measure  $F_M$  for each measurement point because the method is not suitable to measure the  $j_C$ -distribution of an HTS tape or wire. Therefore, it takes long time to evaluate any  $j_C$ -distributions.

\*Corresponding author. Tel./fax: +81-238-26-3789

Email address: [takayama@yz.yamagata-u.ac.jp](mailto:takayama@yz.yamagata-u.ac.jp) (T. Takayama<sup>a</sup>)

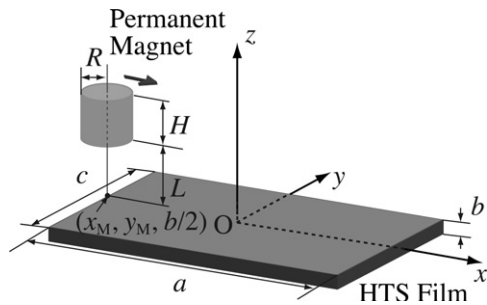


Fig. 1. A schematic view of the scanning permanent magnet method.

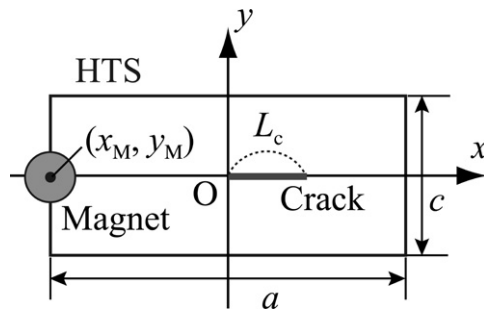


Fig. 2. A crack containing in an HTS film.

Ohshima *et al.* recently propose a modified standard method [7]. In the method, the magnet is placed in relation to an HTS sample at the constant distance between an HTS surface and the magnet bottom and, subsequently, it is moved in the direction parallel to the surface. As a result, they found that a spatial distribution of  $j_C$  can be estimated from a measured an electromagnetic force  $F_z$ . In addition, they conclude that this method is higher speed of the  $j_C$ -distribution measurement than the standard one, and its accuracy hardly change. However, this method has not yet been applied to the crack detection. In the following, this method is called the scanning permanent magnet method.

In order to simulate the standard permanent magnet method, a numerical code was developed for analyzing the time evolution of a shielding current density in an HTS film with a crack [8]. By using the code, the standard method was reproduced for the case with any cracks. The results of computations showed that, the maximum repulsive force  $F_M$  decreases when the magnet approaches the crack. Although the crack size cannot be measured quantitatively, its existence can be identified. As a result, it is found that the standard permanent magnet method can detect a crack.

The purpose of the present study is to reproduce the scanning permanent magnet method by using the above numerical code. Moreover, we investigate whether or not the scanning method is applicable to the crack detection of the film.

## 2. Governing equations and numerical method

In Fig. 1, we show a schematic view of a scanning permanent magnet method. A cylindrical permanent magnet of radius  $R$  and height  $H$  is located above a rectangle-shaped HTS film of width  $a$ , length  $c$ , and thickness  $b$ . In addition, a distance between a magnet bottom and a film surface is denoted by  $L$ .

Throughout the present study, we use the Cartesian coordinate system ( $O : e_x, e_y, e_z$ ), where the  $z$ -axis is parallel to the thickness direction and the origin  $O$  is the centroid of the film. In terms of the coordinate system, the symmetry axis of the permanent magnet can be expressed as  $(x, y) = (x_M, y_M)$ . For characterizing the strength of the magnet, we use a magnetic flux density  $B_F$  at  $(x, y, z) = (0, 0, b/2)$  for the distance  $L$ . On the other hand, we assume an HTS film containing a crack. If a crack is contained in the film, a rectangle cross-section  $\Omega$  of the film has not only the outer boundary  $C_0$  but the inner boundary  $C_1$ . Moreover, a normal unit vector and a tangential unit vector on  $C_1$  are denoted by  $\mathbf{n}$  and  $\mathbf{t}$ , respectively.

As usual, we assume the thin-layer approximation [9]: the thickness of an HTS film is sufficiently thin that a shielding current density can hardly flow in the thickness direction. The shielding current density  $\mathbf{j}$  is closely related to the electric field  $\mathbf{E}$  through the  $J$ - $E$  constitutive equation:  $\mathbf{E} = E(|\mathbf{j}|)[\mathbf{j}/|\mathbf{j}|]$ . As the function  $E(j)$ , we use the power law:  $E(j) = E_C[j/j_C]^N$ , where  $E_C$  is the critical electric field, and  $N$  is a constant.

Under the above assumptions, the shielding current density  $\mathbf{j}$  can be written as  $\mathbf{j} = (2/b)(\nabla S \times \mathbf{e}_z)$  and the time evolution of a scalar function  $S(\mathbf{x}, t)$  is governed by the following integro-differential equation [9]:

$$\mu_0 \partial_t (\hat{W}S) + \partial_t \langle \mathbf{B} \cdot \mathbf{e}_z \rangle + (\nabla \times \mathbf{E}) \cdot \mathbf{e}_z = 0, \quad (1)$$

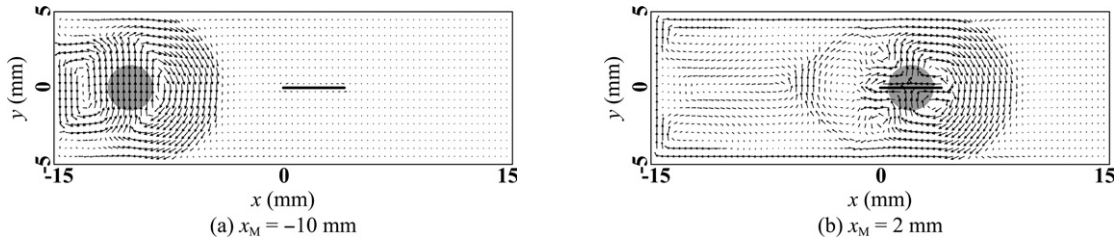


Fig. 3. Spatial distributions of the shielding current density  $\mathbf{j}$  for the case with  $L_c = 4$  mm and  $y_M = 0$  mm. Here, the thick line and the shaded region indicate the crack and the magnet, respectively.

where  $\langle \rangle$  is an average operator over the thickness, and  $\hat{W}S$  is defined by  $\hat{W}S \equiv \iint_{\Omega} Q(|\mathbf{x} - \mathbf{x}'|)S(\mathbf{x}', t)d^2\mathbf{x}' + (2/b)S(\mathbf{x}, t)$ . Here,  $\mathbf{x}$  and  $\mathbf{x}'$  are position vectors in the  $xy$ -plane. The explicit form of  $Q(r)$  is described in [9]. Furthermore, in order to characterize the magnet which the direction of the magnetization is  $z$ -axis, we apply a cylindrical current sheet instead of the magnet.

The initial and boundary conditions to (1) are assumed as follows:  $S = 0$  at  $t = 0$ ,  $S = 0$  on  $C_0$ ,  $\partial S/\partial s = 0$  on  $C_1$  and  $\int_{C_1} \mathbf{E} \cdot \mathbf{t} ds = 0$ . By applying the finite element method and the backward Euler method to the initial-boundary-value problem of (1), the problem is reduced to the nonlinear boundary-value problem. By using the Newton method, it is transformed by simultaneous linear equations. Note that the left hand side  $\int_{C_1} \mathbf{E} \cdot \mathbf{t} ds$  of the boundary condition does not vanish numerically. This is mainly because, in discretizing the initial-boundary-value problem of (1), the boundary condition  $\int_{C_1} \mathbf{E} \cdot \mathbf{t} ds = 0$  is included in the weak form by discretizing the initial-boundary-value problem. For this reason, we adopt the virtual voltage method [10] proposed by Kamitani *et al.*

Under a numerical method, a numerical code is developed for analyzing the time evolution of a shielding current density  $\mathbf{j}$  in an HTS film with a crack.

Throughout the present study, the geometrical and physical parameters are fixed as follows:  $a = 30$  mm,  $c = 10$  mm,  $b = 1$   $\mu\text{m}$ ,  $R = 1.5$  mm,  $H = 3$  mm,  $E_C = 0.1$  mV/m,  $N = 30$ ,  $B_F = 0.3$  T, and  $L = 0.5$  mm. We assume that the  $j_C$ -distribution of the film is uniform, and its value is given by  $j_C = 1$  MA/cm<sup>2</sup>. Also, the crack is assumed to be parallel to  $x$ -axis and its shape is assumed to be a line segment (see Fig. 2). The left endpoint of the crack is taken at the origin  $O$  and the crack size is given by  $L_c$ .

### 3. Simulation of scanning permanent magnet method

Let us first investigate the behavior of the shielding current density  $\mathbf{j}$ . A typical example is shown in Fig. 3 (a) and (b). Here, an arrow indicates the direction and the magnitude of the shielding current density  $\mathbf{j}$ . In Fig. 3(a), the  $\mathbf{j}$ -distribution becomes clockwise on the right side of the magnet (the direction in which the magnet moves), whereas  $\mathbf{j}$ -distribution is counterclockwise on the opposite side. In Fig. 3(b), number of the eddy current increases for affecting  $\mathbf{j}$  significantly.

Next, we investigate whether or not the crack size/position can be detected by using the scanning permanent magnet method. To this end, we calculate a dependence of of an electromagnetic force  $F_z(L_c)$  on the magnet position  $x_M$ . Throughout the present study, the magnet is moved from left end of the film to right: the magnet position is controlled as  $x_M(t) = -a/2 + vt$ . Here, the speed  $v$  of the magnet is fixed as  $v = 2$  mm/s. Otherwise, in order to take a relatively large value near the crack, we define the force difference  $\Delta F_z(L_c) (\equiv F_z(L_c) - F_z(0))$ , where  $F_z(0)$  denotes the electromagnetic force  $F_z$  for the case without crack.

In Fig. 4, we show the dependences of the force difference  $\Delta F_z$  on the magnet position  $x_M$  for the case with the various values of crack size  $L_c$ . We see from this figure that, for  $-15 \text{ mm} \leq x_M \lesssim -5 \text{ mm}$ , the force difference  $\Delta F_z$  almost vanishes, whereas, for  $x_M \gtrsim -5 \text{ mm}$ , the behavior of  $\Delta F_z$  significantly changes due to the crack. Specifically, when the magnet approaches the left point  $(x, y) = (0 \text{ mm}, 0 \text{ mm})$  of the crack, a repulsive force  $F_r$  acts on the film. On the other hand, an attractive force  $F_a$  is generated near the right point  $(x, y) = (L_c, 0 \text{ mm})$ . In fact, we evaluate the maximum absolute values of  $F_r$  and  $F_a$  at  $x_M = x_r$  and  $x_M = x_a$ .

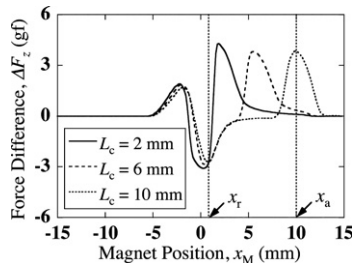


Fig. 4. Dependences of the force difference  $\Delta F_z$  on the magnet position  $x_M$  for the case with  $y_M = 0$  mm.

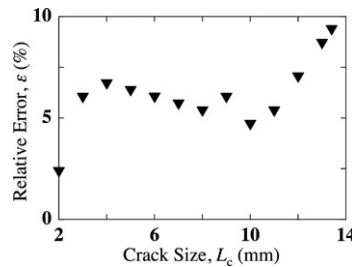


Fig. 5. Dependence of the relative error  $\varepsilon$  on the crack size  $L_c$  for the case with  $y_M = 0$  mm.

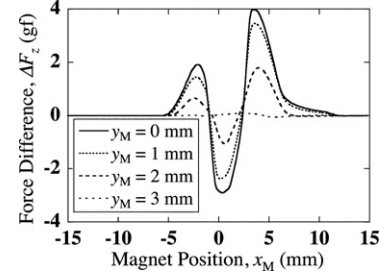


Fig. 6. Dependences of the force difference  $\Delta F_z$  on the magnet position  $x_M$  for the case with  $L_c = 4$  mm.

For example, we get  $x_r = 0.7$  mm and  $x_a = 10$  mm for the case with  $L_c = 10$  mm (see Fig. 4). This result implies that the crack size can be detected from two forces,  $F_r$  and  $F_a$ .

In order to quantitatively evaluate the crack size  $L_c$ , we define the relative error  $\varepsilon \equiv 2|L_c^* - L_c|/a$ . Here  $L_c^*$  is an evaluated value of the crack size, it defines  $L_c^* \equiv |x_a - x_r|$ . In Fig. 5, we show the dependence of the relative error  $\varepsilon$  on the crack size  $L_c$ . We see from this figure that the value of the relative error is 10 % or less for  $2 \text{ mm} \leq L_c \leq 13.4 \text{ mm}$ , and the accuracy of the crack-size detection is degraded for long crack. Incidentally, the relative error  $\varepsilon$  cannot be calculated because we cannot obtain the value of  $F_r$  for  $L_c = 13.4$  mm. From this result, although the crack size can be roughly detected, the crack cannot be detected near the film edge.

Finally, we investigate the detectability of the crack position. To this end, the spatial distributions of force difference  $\Delta F_z$  are calculated as a function of the magnet position  $x_M$  for various  $y_M$  and are depicted in Fig. 6. From this figure, the repulsive force  $F_r$  and the attractive force  $F_a$  decrease when the symmetry  $y$ -axis of the magnet approaches the top edge of the film. In addition, we found that  $F_r$  and  $F_a$  become the maximum value only when the magnet is located above the crack.

We conclude that, by measuring the  $F_z$ -distribution in over all HTS surface, the crack can be detected by means of the scanning permanent magnet method. In the future, we examine the applicable to the detection of the crack direction. Since experimental results of the crack detection does not exist yet by using the scanning method, we will compare the experimental results with numerical ones.

## References

- [1] J. H. Claassen, M. E. Reeves, R. J. Soulen, Jr., A contactless method for measurement of the critical current density and critical temperature of superconducting films, *Rev. Sci. Instrum.* 62 (1999) 996-1004.
- [2] K. Nakao, T. Machi, S. Miyata, T. Muroga, A. Ibi, T. Watanabe et al., Non-destructive characterization of long coated conductors using a Hall sensor array, *Physica C* 445-448 (2006) 669-672.
- [3] M. Zehetmayer, R. Fuger, R. Hengstberger, M. Kitzmantel, M. Eisterer, H. W. Weber, Modified magnetoscan technique for assessing inhomogeneities in the current flow of coated conductors - Theory and experiment, *Physica C* 460-462 (2007) 158-161.
- [4] S. Ohshima, K. Takeishi, A. Saito, M. Mukaida, Y. Takano, T. Nakamura et al., A simple measurement technique for critical current density by using a permanent magnet, *IEEE Trans Appl Supercond* 15 (2005) 2911-2914.
- [5] S. Ikuno, T. Takayama, A. Kamitani, K. Takeishi, A. Saito, S. Ohshima, Analysis of measurement method for critical current density by using permanent magnet, *IEEE Trans Appl Supercond* 19 (2009) 3750-3754.
- [6] S. Ohshima, K. Umezumi, K. Hattori, H. Yamada, A. Saito, T. Takayama et al., Detection of critical current distribution of YBCO-coated conductors using permanent magnet method. *IEEE Trans Appl Supercond* 21 (2011) 3385-3388.
- [7] K. Hattori, A. Saito, Y. Takano, H. Yamada, T. Takayama, A. Kamitani et al., Detection of smaller  $J_c$  region and damage in YBCO coated conductors by using permanent magnet method. *Physica C* 471 (2011) 1033-1035.
- [8] T. Takayama, A. Kamitani, A. Saitoh, H. Nakamura, Numerical investigation on accuracy and resolution of contactless methods for measuring  $j_c$  in high-temperature superconducting film: inductive method and permanent magnet method, *Plasma and Fusion Research* 6 (2012) 2405017.
- [9] A. Kamitani, S. Ohshima, Magnetic shielding analysis of axisymmetric HTS plates in mixed state, *IEICE Trans Electron* E82-C (1999) 766-773.
- [10] A. Kamitani, T. Takayama, Numerical simulation of shielding current density in high-temperature superconducting film: influence of film edge on permanent magnet method, *IEEE Trans Magn* 48 (2012) 727-730.